

1.16

FIRST-PRINCIPLES MODELING OF PHASE EQUILIBRIA

Axel van de Walle and Mark Asta
Northwestern University, Evanston, IL, USA

First-principles approaches to the modeling of phase equilibria rely on the integration of accurate quantum-mechanical total-energy calculations and statistical-mechanical modeling. This combination of methods makes possible parameter-free predictions of the finite-temperature thermodynamic properties governing a material's phase stability. First-principles, computational-thermodynamic approaches have found increasing applications in phase diagram studies of a wide range of semiconductor, ceramic and metallic systems. These methods are particularly advantageous in the consideration of previously unexplored materials, where they can be used to ascertain the thermodynamic stability of new materials before they are synthesized, and in situations where direct experimental thermodynamic measurements are difficult due to constraints imposed by kinetics or metastability.

1. First-Principles Calculations of Thermodynamic Properties: Overview

At finite temperature (T) and pressure (P) thermodynamic stability is governed by the magnitude of the Gibbs free energy (G):

$$G = E - TS + PV \quad (1)$$

where E , S and V denote energy, entropy and volume, respectively. In principle, the formal statistical-mechanical procedure for calculating G from first-principles is well defined. Quantum-mechanical calculations can be performed to compute the energy $E(s)$ of different microscopic states (s) of a system, which then must be summed up in the form of a partition function (Z):

$$Z = \sum_s \exp[-E(s)/k_B T] \quad (2)$$

from which the free energy is derived as $F = E - TS = -k_B T \ln Z$, where k_B is Boltzmann's constant.

Figure 1(a) illustrates, for the case of a disordered crystalline binary alloy, the nature of the disorder characterizing a representative finite-temperature atomic structure. This disorder can be characterized in terms of the *configurational* arrangement of the elemental species over the sites of the underlying parent lattice, coupled with the *displacements* characterizing positional disorder. In principle, the sum in Eq. (2) extends over all configurational and displacive states accessible to the system, a phase space that is astronomically large for a realistic system size. In practice, the methodologies of atomic-scale molecular dynamics (MD) and Monte Carlo (MC) simulations, coupled with thermodynamic integration techniques (Kofke and Frenkel, de Koning, Chapter 2), reduce the complexity of a free energy calculation to a more tractable problem of sampling on the order of several to tens of thousands of representative states.

Electronic density-functional theory (DFT) provides an accurate quantum-mechanical framework for calculating the relative energetics of competing atomic structures in solids, liquids and molecules for a wide range of materials classes (Kaxiras, Chapter 1). Due to the rapid increase in computational cost with system size, however, DFT calculations are typically limited to structures containing fewer than ≈ 1000 atoms, while *ab initio* MD simulations (Scheffler, Chapter 1) are practically limited to time scales of less than ≈ 1 ns. For liquids or compositionally ordered solids, where the time scales for structural rearrangements (displacive in the latter case, configurational and displacive

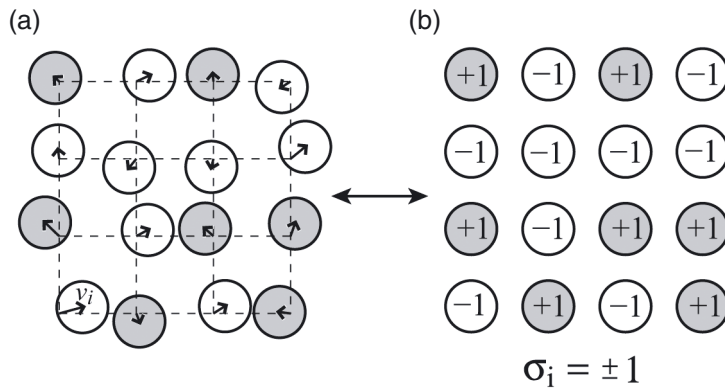


Figure 1. (a) Disordered crystalline alloy. The state of the alloy is characterized both by the atomic displacements v_i and the occupation of each lattice site. (b) Mapping of the real alloy onto a lattice model characterized by occupation variables σ_i describing the identity of atoms on each of the lattice sites.

in the former) are sufficiently fast, and the size of periodic cells required to accurately model the atomic structure are relatively small, DFT-based MD methods have found direct applications in the calculation of finite-temperature thermodynamic properties [1, 2]. For crystalline solids containing both positional and concentrated compositional disorder, however, direct applications of DFT to the calculation of free energies remains intractable; the time scales for configurational rearrangements are set by solid-state diffusion, ruling out direct application of MD, and the necessary system sizes required to accurately model configurational disorder are too large to permit direct application of DFT as the basis for MC simulations. Effective strategies have nonetheless been developed for bridging the size and time-scale limitations imposed by DFT in the first-principles computation of thermodynamic properties for disordered solids. The approach involves exploitation of DFT methods as a framework for parameterizing classical potentials and coarse-grained statistical models. These models serve as efficient “effective Hamiltonians” in direct simulation-based calculations of thermodynamic properties; they can also function as useful reference systems for thermodynamic-integration calculations.

2. Thermodynamics of Compositionally Ordered Solids

In an ordered solid thermal fluctuations take the form of electronic excitations and lattice vibrations and, accordingly, the free energy can be written as $F = E_0 + F_{\text{elec}} + F_{\text{vib}}$, where E_0 is the absolute zero total energy while F_{elec} and F_{vib} denote electronic and vibrational free energy contributions, respectively. This section is devoted to the calculation of the electronic and vibrational contributions most commonly considered in phase-diagram calculations under the assumption that electron–phonon interactions are negligible (i.e., F_{elec} and F_{vib} are simply additive).

To account for electronic excitations, electronic DFT (Kaxiras, Chapter 1) can be extended to nonzero temperatures by allowing for partial occupations of the electronic states [3]. Within this framework, the electronic contribution to the free energy $F_{\text{elec}}(T)$ at temperature T can be decomposed as*

$$F_{\text{elec}}(T) = E_{\text{elec}}(T) - E_{\text{elec}}(0) - TS_{\text{elec}}(T) \quad (3)$$

*Equations (3)–(5) also assume that both the electronic charge density and the electronic density of states can be considered temperature-independent.

obtained by finding the eigenvalues of the so-called $3n \times 3n$ dynamical matrix of the system:

$$D(k) = \sum_l e^{i2\pi(k \cdot l)} \begin{pmatrix} \frac{\Phi_{(11)}^{(0l)}}{\sqrt{M_1 M_1}} & \cdots & \frac{\Phi_{(1n)}^{(0l)}}{\sqrt{M_1 M_n}} \\ \vdots & \ddots & \vdots \\ \frac{\Phi_{(n1)}^{(0l)}}{\sqrt{M_n M_1}} & \cdots & \frac{\Phi_{(nn)}^{(0l)}}{\sqrt{M_n M_n}} \end{pmatrix} \quad (9)$$

for all vectors k in the first Brillouin zone. The resulting eigenvalues $\lambda_b(k)$ for $b = 1, \dots, 3n$, provide the frequencies of the normal modes through $\nu_b(k) = 1/2\pi (\sqrt{\lambda_b(k)})$. This information for all k is conveniently summarized by $g(\nu)$, the phonon density of states (DOS), which specifies the number of modes of oscillation having a frequency lying in the infinitesimal interval $[\nu, \nu + d\nu]$. The vibrational free energy (per unit cell) F_{vib} is then given by

$$F_{\text{vib}} = k_B T \int_0^\infty \ln \left(2 \sinh \left(\frac{h\nu}{2k_B T} \right) \right) g(\nu) d\nu \quad (10)$$

where h is Planck's constant and k_B is Boltzman's constant. The associated vibrational entropy S_{vib} of the system can be obtained from the well-known thermodynamic relationship $S_{\text{vib}} = -\partial F_{\text{vib}}/\partial T$. The high temperature limit (which is also the classical limit) of Eq. (10) is often a good approximation over the range of temperature of interest in solid-state phase diagram calculations

$$F_{\text{vib}} = k_B T \int_0^\infty \ln \left(\frac{h\nu}{k_B T} \right) g(\nu) d\nu.$$

The high temperature limit of the vibrational entropy difference between two phases is often used as measure of the magnitude of the effect of lattice vibrations on phase stability. It has the advantage of being temperature-independent, thus allowing a unique number to be reported as a measure of vibrational effects. Figure 2 (from [5]) illustrates the use of the above formalism to assess the relative phase stability of the θ and θ' phases responsible for precipitation hardening in the Al–Cu system. Interestingly, accounting for lattice vibrations is crucial in order for the calculations to agree with the experimentally observed fact that the θ phase is stable at typical processing temperatures ($T > 475$ K).

A simple improvement over the harmonic approximation, called the quasi-harmonic approximation, is obtained by employing volume-dependent force constant tensors. This approach maintains all the computational advantages of the harmonic approximation while permitting the modeling of thermal expansion. The volume dependence of the phonon frequencies induced by the volume dependence of the force constants is traditionally described by the Grüneisen parameter $\gamma_{kb} = -\partial \ln \nu_b(k)/\partial \ln V$. However, for the purpose of

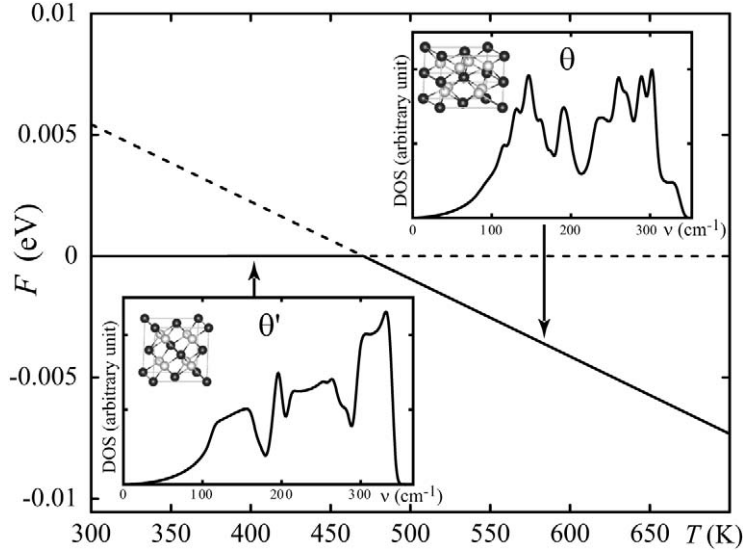


Figure 2. Temperature-dependence of the free energy of the θ and θ' phases of the Al_2Cu compound. Insets show the crystal structures of each phase and the corresponding phonon density of states. Dashed lines indicate region of metastability and the θ phase is seen to become stable above about 475 K. (Adapted from Ref. [5] with the permission of the authors.)

modeling thermal expansion, it is more convenient to directly parametrize the volume-dependence of the free energy itself. This dependence has two sources: the change in entropy due to the change in the phonon frequencies and the elastic energy change due to the expansion of the lattice:

$$F(T, V) = E_0(V) + F_{\text{vib}}(T, V) \quad (11)$$

where $E_0(V)$ is the energy of a motionless lattice whose unit cell is constrained to remain at volume V , while $F_{\text{vib}}(T, V)$ is the vibrational free energy of a harmonic system constrained to remain with a unit cell volume V at temperature T . The equilibrium volume $V^*(T)$ at temperature T is obtained by minimizing $F(T, V)$ with respect to V . The resulting free energy $F(T)$ at temperature T is then given by $F(T, V^*(T))$. The quasiharmonic approximation has been shown to provide a reliable description of thermal expansion of numerous elements up to their melting points, as illustrated in Fig. 3.

First-principles calculations can be used to provide the necessary input parameters for the above formalism. The so-called direct force method proceeds by calculating, from first principles, the forces experienced by the atoms in response to various imposed displacements and by determining the value of the force constant tensors that match these forces through a least-squares fit.

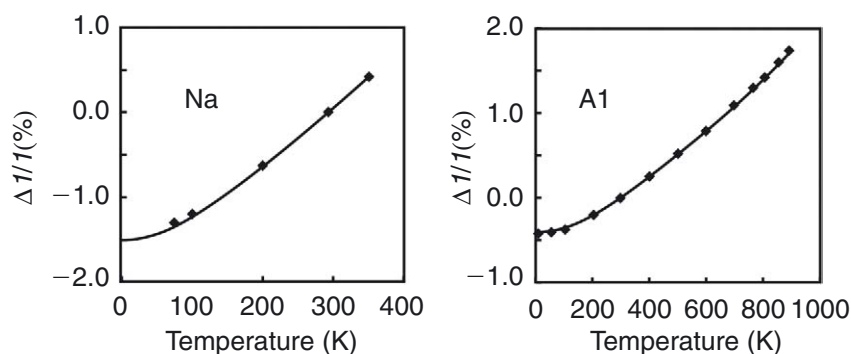


Figure 3. Thermal expansion of selected metals calculated within the quasiharmonic approximation. (Reproduced from Ref. [6] with the permission of the authors.)

Note that the simultaneous displacements of the periodic images of each displaced atom due to the periodic boundary conditions used in most *ab initio* methods typically requires the use of a supercell geometry, in order to be able to sample all the displacements needed to determine the force constants. While the number of force constants to be determined is in principle infinite, in practice, it can be reduced to a manageable finite number by noting that the force constant tensor associated with two atoms that lie farther than a few nearest neighbor shells can be accurately neglected for many systems. Alternatively, linear response theory (Rabe, Chapter 1) can be used to calculate the dynamical matrix $D(k)$ directly using second-order perturbation theory, thus circumventing the need for supercell calculations. Linear response theory is also particularly useful when a system is characterized by non-negligible long-range force-constants, as in the presence of Fermi-surface instabilities or long-ranged electrostatic contributions.

The above discussion has centered around the application of harmonic (or quasiharmonic) approximations to the statistical modeling of vibrational contributions to free energies of solids. While harmonic theory is known to be highly accurate for a wide class of materials, important cases exist where this approximation breaks down due to large anharmonic effects. Examples include the modeling of ferroelectric and martensitic phase transformations where the high-temperature phases are often dynamically unstable at zero temperature, i.e., their phonon spectra are characterized by unstable modes. In such cases, effective Hamiltonian methods have been developed to model structural phase transitions from first principles (Rabe, Chapter 1). Alternatively, direct application of *ab initio* molecular-dynamics offers a general framework for modeling thermodynamic properties of anharmonic solids [1, 2].

3. Thermodynamics of Compositionally Disordered Solids

We now relax the main assumption made in the previous section, by allowing atoms to exit the neighborhood of their local equilibrium position. This is accomplished by considering every possible way to arrange the atoms on a given lattice. As illustrated in Fig. 1(b), the state of order of an alloy can be described by occupation variables σ_i specifying the chemical identity of the atom associated with lattice site i . In the case of a binary alloy, the occupations are traditionally chosen to take the values $+1$ or -1 , depending on the chemical identity of the atom.

Returning to Eq. (2), all the thermodynamic information of a system is contained in its partition function Z and in the case of a crystalline alloy system, the sum over all possible states of the system can be conveniently factored as follows:

$$Z = \sum_{\sigma} \sum_{v \in \sigma} \sum_{e \in v} \exp[-\beta E(\sigma, v, e)] \quad (12)$$

where $\beta = (k_B T)^{-1}$ and where

- σ denotes a configuration (i.e., the vector of all occupation variables);
- v denotes the displacement of each atom away from its local equilibrium position;
- e is a particular electronic state when the nuclei are constrained to be in a state described by σ and v ; and
- $E(\sigma, v, e)$ is the energy of the alloy in a state characterized by σ , v and e .

Each summation defines an increasingly coarser level of hierarchy in the set of microscopic states. For instance, the sum over v includes all displacements such that the atoms remain close to the undistorted configuration σ . Equation (12) implies that the free energy of the system can be written as

$$F(T) = -k_B T \ln \left(\sum_{\sigma} \exp[-\beta F(\sigma, T)] \right) \quad (13)$$

where $F(\sigma, T)$ is nothing but the free energy of an alloy with a fixed atomic configuration, as obtained in the previous section

$$F(\sigma, T) = -k_B T \ln \left(\sum_{v \in \sigma} \sum_{e \in v} \exp[-\beta E(\sigma, v, e)] \right) \quad (14)$$

The so-called ‘‘coarse graining’’ of the partition function illustrated by Eq. (13) enables, in principle, an exact mapping of a real alloy onto a simple lattice model characterized by the occupation variables σ and a temperature-dependent Hamiltonian $F(\sigma, T)$ [7, 8].

Although we have reduced the problem of modeling the thermodynamic properties of configurationally disordered solids to a more tractable calculation for a lattice model, the above formalism would still require the calculation of the free energy for every possible configuration σ , which is computationally intractable. Fortunately, the configurational dependence of the free energy can often be parametrized using a convenient expansion known as a cluster expansion [7, 9]. This expansion takes the form of a polynomial in the occupation variables

$$F(\sigma, T) = J_\emptyset + \sum_i J_i \sigma_i + \sum_{i,j} J_{ij} \sigma_i \sigma_j + \sum_{i,j,k} J_{ijk} \sigma_i \sigma_j \sigma_k + \dots$$

where the so-called effective cluster interactions (ECI) $J_\emptyset, J_i, J_{ij}, \dots$, need to be determined. The cluster expansion can be recast into a form which exploits the symmetry of the lattice by regrouping the terms as follows

$$F(\sigma, T) = \sum_\alpha m_\alpha J_\alpha \left\langle \prod_{i \in \alpha'} \sigma_i \right\rangle$$

where α is a cluster (i.e., a set of lattice sites) and where the summation is taken over all clusters that are symmetrically distinct while the average $\langle \dots \rangle$ is taken over all clusters α' that are symmetrically equivalent to α . The multiplicity m_α weight each term by the number of symmetrically equivalent clusters in a given reference volume (e.g., a unit cell). While the cluster expansion is presented here in the context of binary alloys, an extension to multicomponent alloys (where σ_i can take more than two different values) is straightforward [9].

It can be shown that when *all* clusters α are considered in the sum, the cluster expansion is able to represent any function of configuration σ by an appropriate selection of the values of J_α . However, the real advantage of the cluster expansion is that, for many systems, it is found to converge rapidly. An accuracy that is sufficient for phase diagram calculations can often be achieved by keeping only clusters α that are relatively compact (e.g., short-range pairs or small triplets, as illustrated in the left panel of Fig. 4). The unknown parameters of the cluster expansion (the ECI J_α) can then be determined by fitting them to $F(\sigma, T)$ for a relatively small number of configurations σ obtained from first-principles computations. Once the ECI have been determined, the free energy of the alloy for any given configuration can be quickly calculated, making it possible to explore a large number of configurations without recalculating their free energy from first principles for each of them.

In some applications the development of a converged cluster expansion can be complicated by the presence of long-ranged interatomic interactions mediated by electronic-structure (Fermi-surface), electrostatic and/or elastic effects. Long-ranged interactions lead to an increase in the number of ECIs

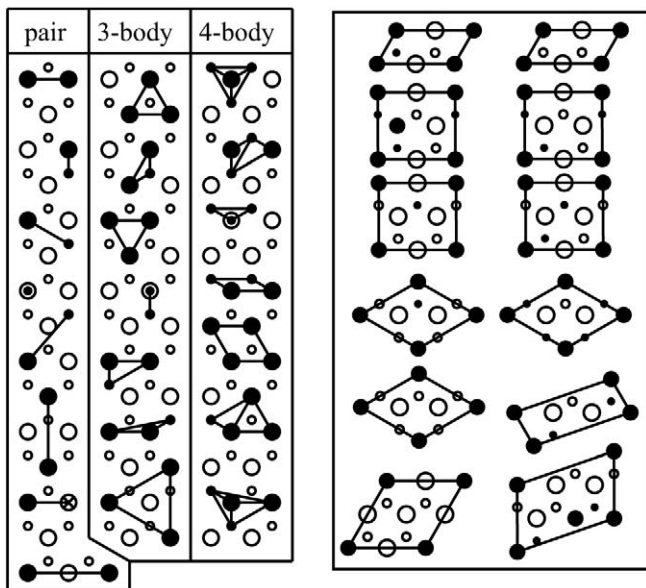


Figure 4. Typical choice of clusters (left) and structures (right) used for the construction of a cluster expansion on the hcp lattice. Big circles, small circles and crosses represent consecutive close-packed planes of the hcp lattice. Concentric circles represent two sites, one above the other in the $[0001]$ direction. The unit cell of the structures (right) along the (0001) plane is indicated by lines while the third lattice vector, along $[0001]$, is identical to the one of the hcp primitive cell. (Adapted, with the permission of the authors, from Ref. [10], a first-principles study of the metastable hcp phase diagram of the Ag–Al system.)

that must be computed, and a concomitant increase in the number of configurations that must be sampled to derive them. For metals it has been demonstrated how long-ranged electronic interactions can be derived from perturbation theory using coherent-potential approximations to the electronic structure of a configurationally disordered solid as a reference state [11]. Effective approaches to modeling long-ranged elastically mediated interactions have also been formulated [12]. Such elastic effects are known to be particularly important in describing the thermodynamics of mixtures of species with very large differences in atomic “size”.

The cluster expansion tremendously simplifies the search for the lowest energy configuration at each composition of the alloy system. Determining these ground states is important because they determine the general topology of the alloy phase diagram. Each ground state is typically associated with one of the stable phases of the alloy system. There are three main approaches to identify the ground states of an alloy system.

With the enumeration method, all the configurations whose unit cell contains less than a given number of atoms are enumerated and their energy

is quickly calculated using the value of $F(\sigma, 0)$ predicted from the cluster expansion. The energy of each structure can then be plotted as a function of its composition (see Fig. 5) and the points touching the lower portion of the convex hull of all points indicate the ground states. While this method is approximate, as it ignores ground states with unit cell larger than the given threshold, it is simple to implement and has been found to be quite reliable, thanks to the fact that most ground states indeed have a small unit cell.

Simulated annealing offers another way to find the ground states. It proceeds by generating random configurations via MC simulations using the Metropolis algorithm (G. Gilmer, Chapter 2) that mimic the ensemble sampled in thermal equilibrium at a given temperature. As the temperature is lowered, the simulation should converge to the ground state. Thermal fluctuations are used as an effective means of preventing the system from getting trapped in local minima of energy. While the constraints on the unit cell size are considerably relaxed relative to the enumeration method, the main disadvantage of this method is that, whenever the simulation cell size is not an exact multiple of the ground state unit cell, artificial defects will be introduced in the simulation that need to be manually identified and removed. Also, the risk of obtaining local rather than global minima of energy is not negligible and must be controlled by adjusting the rate of decay of the simulation temperature.

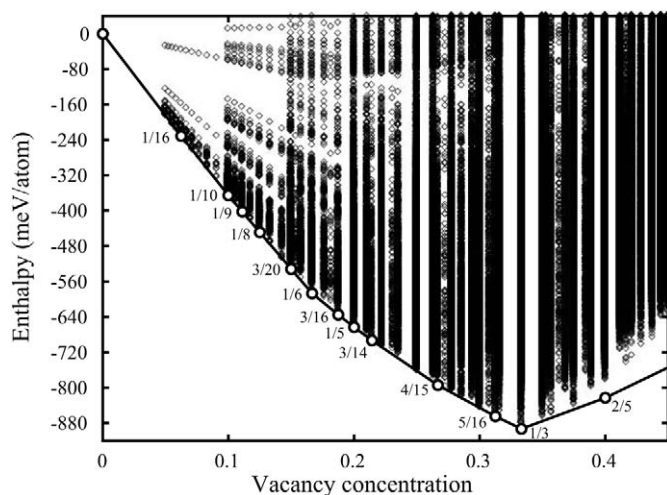


Figure 5. Ground state search using the enumeration method in the $\text{Sc}_x\text{-Vacancy}_{1-x}\text{S}$ system. Diamonds represent the formation energies of about 3×10^6 structures, predicted from a cluster expansion fitted to LDA energies. The ground states, indicated by open circles, are the structures whose formation energy touches the convex hull (solid line) of all points. (Reproduced from Ref. [13], with the permission of the authors.)

Finally, there exists an exact, although computational demanding, algorithm to identify the ground states [14]. This approach relies on the fact that the cluster expansion is linear in the correlations $\sigma_\alpha \equiv \langle \prod_{i \in \alpha'} \sigma_i \rangle$. Moreover, it can be shown that the set of correlations σ_α that correspond to “real” structures can be defined by a set of linear inequalities. These inequalities are the result of lattice-specific geometric constraints and there exists systematic methods to generate them [14]. As an example of such constraints, consider the fact that it is impossible to construct a binary configuration on a triangular lattice where the nearest neighbor pair correlations take the value -1 (i.e., where all nearest neighbors are between unlike atomic species). Since both the objective function and the constraints are linear in the correlations, linear programming techniques can be used to determine the ground states. The main difficulties associated with this method is the fact that the resulting linear programming problem involves a number of dimensions and a number of inequalities that grows exponentially fast with the range of interactions included in the cluster expansion.

Once the ground states have been identified, thermodynamic properties at finite temperature must be obtained. Historically, the infinite summation defining the alloy partition function has been approximated through various mean-field methods [7, 14]. However, the difficulties associated with extending such methods to systems with medium to long-ranged interactions, and the increase in available computational power enabling MC simulations to be directly applied, have led to reduced reliance upon these techniques more recently.

MC simulations readily provide thermodynamic quantities such as energy or composition by making use of the fact that averages over an infinite ensemble of microscopic states can be accurately approximated by averages over a finite number of states generated by “importance” sampling. Moreover, quantities such as the free energy, which cannot be written as ensemble averages, can nevertheless be obtained via *thermodynamic integration* (Frenkel, Chapter 2; de Koning, Chapter 2) using standard thermodynamic relationships to rewrite the free energy in terms of integrals of quantities that can be obtained via ensemble averages. For instance, since energy $E(T)$ and free energy $F(T)$ are related through $E(T) = \partial(F(T)/T)/\partial(1/T)$ we have

$$\frac{F(T)}{T} - \frac{F(T_0)}{T_0} = \int_{T_0}^T \frac{E(T)}{T^2} dT \quad (15)$$

and free energy differences can therefore be obtained from MC simulations providing $E(T)$. Figures 6 and 7 show two phase diagrams obtained by combining first principles calculations, the cluster expansion formalism and MC simulations, an approach which offers the advantage of handling, in a

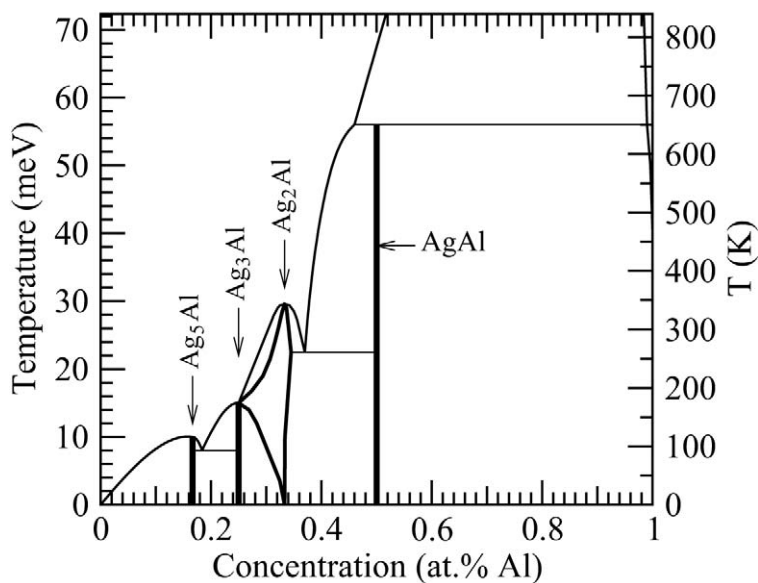


Figure 6. Calculated composition–temperature phase diagram for a metastable hcp Ag–Al alloy. Note that the cluster expansion formalism enables a unified treatment of both solid solutions and ordered compounds. (Reproduced from Ref. [10], with the permission of the authors.)

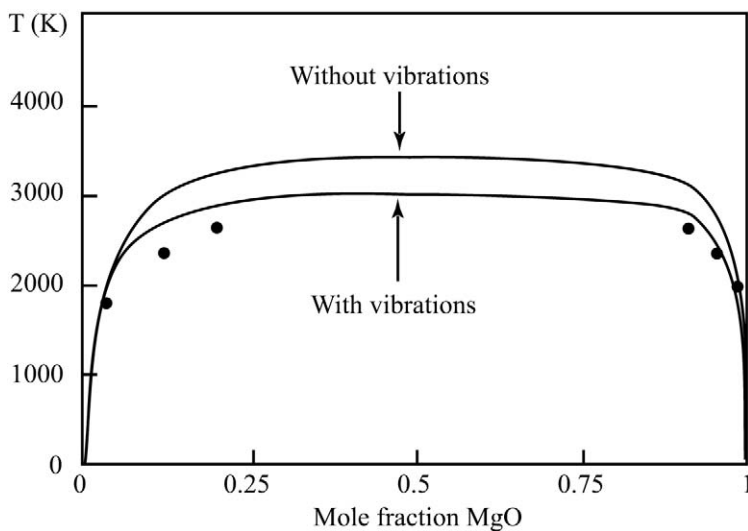


Figure 7. Calculated composition–temperature solid-state phase diagram for a rocksalt-type CaO–MgO alloy. The inclusion of lattice vibrations via the coarse-graining formalism is seen to substantially improve in agreement with experimental observations (filled circles). (Reproduced from Ref. [15], with the permission of the authors.)

unified framework, both ordered phases (with potential thermal defects) and disordered phases (with potential short-range order).

4. Liquids and Melting Transitions

While first-principles thermodynamic methods have found the widest application in studies of solids, recent progress has been realized also in the development and application of methods for *ab initio* calculations of solid–liquid phase boundaries. This section provides a brief overview of such methods, based upon the application of thermodynamic integration methods within the framework of *ab initio* molecular dynamics simulations.

Consider the *ab initio* calculation of the melting point for an elemental system, as was first demonstrated by Sugino and Car [1] in an application to elemental Si. The approach is based on the use of thermodynamic-integration methods to compute temperature-dependent free energies for bulk solid and liquid phases. Let $U_1(r_1, r_2, \dots, r_N)$ denote the DFT potential energy for a collection of ions at positions (r_1, \dots, r_N) , while $U_0(r_1, r_2, \dots, r_N)$ corresponds to the energy of the same collection of ions described by a reference classical-potential model. We suppose that the free energy of the reference system, F_0 , has been accurately calculated, either analytically (as in the case of an Einstein crystal) or using the atomistic simulation methods reviewed by Kofke and Frenkel in Chapter 2. We proceed to calculate the *difference* $F_1 - F_0$ between the DFT free energy (F_1) and F_0 employing the statistical-mechanical relation:

$$F_1 - F_0 = \int_0^1 d\lambda \left\langle \frac{dU_\lambda}{d\lambda} \right\rangle_\lambda = \int_0^1 d\lambda \langle U_1 - U_0 \rangle_\lambda \quad (16)$$

where the brackets $\langle \dots \rangle_\lambda$ denote an average over the ensemble generated by the potential energy $U_\lambda = \lambda U_1 + (1 - \lambda)U_0$. In practice, $\langle \dots \rangle_\lambda$ can be calculated from a time average over an MD trajectory generated with forces derived from the hybrid energy U_λ . The integral in Eq. (16) is evaluated from results computed for a discrete set of λ values, or from a time average over a simulation where λ is slowly “switched” on from zero to one. Practical applications of this approach rely on the careful choice of the reference system to provide energies that are sufficiently “close” to DFT to allow the ensemble averages in Eq. (16) to be precisely calculated from relatively short MD simulations. It should be emphasized that the approach outlined in this paragraph, when applied to the solid phase, provides a framework for accurately calculating anharmonic contributions to the vibrational free energy.

Figure 8 shows results derived from the above procedure by Sugino and Car [1] in an application to elemental Si (using the Stillinger–Weber potential as a reference system). Temperature-dependent chemical potentials for solid and

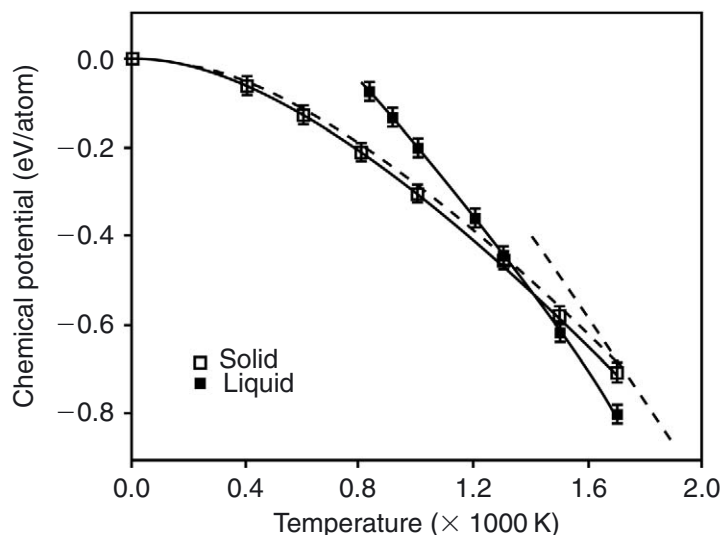


Figure 8. Calculated chemical potential of solid and liquid silicon. Full lines correspond to theory and dashed lines to experiments. (Reproduced from Ref. [1], with the permission of the authors.)

liquid phases (referenced to the zero-temperature free energy of the crystal) are plotted with symbols and are compared to experimental data represented by the dashed lines. It can be seen that the temperature-dependence of the solid and liquid free energies (i.e., the slopes of the curves in Fig. 8) are accurately predicted. Relative to the solid, the liquid chemical potentials are approximately 0.1 eV/atom lower than experiment, leading to a calculated melting temperature that is approximately 300 K lower than the measured value. Comparable and even somewhat higher accuracies have been demonstrated in more recent applications of this approach to the calculation of melting temperatures in elemental metal systems (see, e.g., the references cited in [2]).

The above formalism has been extended as a basis for calculating solid and liquid chemical potentials in binary *mixtures* [2]. In this application, thermodynamic integration for the liquid phase is used to compute the change in free energy accompanying the continuous interconversion of atoms from solute to solvent species. Such calculations form the basis for extracting solute and solvent atom chemical potentials. For the solid phase the vibrational free energy of formation of substitutional impurities is extracted either within the harmonic approximation (along the lines described above) and/or from thermodynamic integration to derive anharmonic contributions. In applications to Fe-based systems relevant to studies of the Earth's core, the approach has been used to compute the equilibrium partitioning of solute atoms between

solid and liquid phases in binary mixtures at pressures that are beyond the range of direct experimental measurements.

5. Outlook

The techniques described in this article provide a framework for computing the thermodynamic properties of elements and alloys from first principles, i.e., requiring, in principle, only the atomic numbers of the elemental constituents as input. In the most favorable cases, these methods have been demonstrated to yield finite-temperature thermodynamic properties with an accuracy that is limited only by the approximations inherent in electronic DFT. For a growing number of metallic alloy systems, such accuracy can be comparable to that achievable in direct measurements of thermodynamic properties. In such cases, *ab initio* methods have found applications as a framework for augmenting the experimental databases that form the basis of “computational-thermodynamics” modeling in the design of alloy microstructure. First-principles methods offer the advantage of being able to provide estimates of thermodynamic properties in situations where direct experimental measurements are difficult due to constraints imposed by sluggish kinetics, metastability or extreme conditions (e.g., high pressures or temperatures). In the development of new materials, first-principles methods can be employed as a framework for rapidly assessing the thermodynamic stability of hypothetical structures before they are synthesized. With the continuing increase in computational power and improvements in the accuracy of first-principles electronic-structure methods, it is anticipated that *ab initio* techniques will find growing applications in predictive studies of phase stability for a wide range of materials systems.

References

- [1] O. Sugino and R. Car, “*Ab initio* molecular dynamics study of first-order phase transitions: melting of silicon,” *Phys. Rev. Lett.*, 74, 1823, 1995.
- [2] D. Alfè, M.J. Gillan, and G.D. Price, “*Ab initio* chemical potentials of solid and liquid solutions and the chemistry of the Earth’s core,” *J. Chem. Phys.*, 116, 7127, 2002.
- [3] N.D. Mermin, “Thermal properties of the inhomogeneous electron gas,” *Phys. Rev.*, 137, A1441, 1965.
- [4] A.A. Maradudin, E.W. Montroll, and G.H. Weiss, *Theory of Lattice Dynamics in the Harmonic Approximation*, 2nd edn., Academic Press, New York, 1971.
- [5] C. Wolverton and V. Ozoliņš, “Entropically favored ordering: the metallurgy of Al_2Cu revisited,” *Phys. Rev. Lett.*, 86, 5518, 2001.
- [6] A.A. Quong and A.Y. Lui, “First-principles calculations of the thermal expansion of metals,” *Phys. Rev. B*, 56, 7767, 1997.

- [7] D. de Fontaine, "Cluster approach to order-disorder transformation in alloys," *Solid State Phys.*, 47, 33, 1994.
- [8] A. van de Walle and G. Ceder, "The effect of lattice vibrations on substitutional alloy thermodynamics," *Rev. Mod. Phys.*, 74, 11, 2002.
- [9] J.M. Sanchez, F. Ducastelle, and D. Gratias, "Generalized cluster description of multicomponent systems," *Physica*, 128A, 334, 1984.
- [10] N.A. Zarkevich and D.D. Johnson, "Predicted hcp Ag–Al metastable phase diagram, equilibrium ground states, and precipitate structure," *Phys. Rev. B*, 67, 064104, 2003.
- [11] G.M. Stocks, D.M.C. Nicholson, W.A. Shelton, B.L. Gyorffy, F.J. Pinski, D.D. Johnson, J.B. Staunton, P.E.A. Turchi, and M. Sluiter, "First Principles Theory of Disordered Alloys and Alloy Phase Stability," In: P.E. Turchi and A. Gonis (eds.), *NATO ASI on Statics and Dynamics of Alloy Phase Transformation*, vol. 319, Plenum Press, New York, p. 305, 1994.
- [12] C. Wolverton and A. Zunger, "An ising-like description of structurally-relaxed ordered and disordered alloys," *Phys. Rev. Lett.*, 75, 3162, 1995.
- [13] G.L. Hart and A. Zunger, "Origins of nonstoichiometry and vacancy ordering in $\text{Sc}_{1-x}\text{S}_x$," *Phys. Rev. Lett.*, 87, 275508, 2001.
- [14] F. Ducastelle, *Order and Phase Stability in Alloys.*, Elsevier Science, New York, 1991.
- [15] P.D. Tepesch, A.F. Kohan, and G.D. Garbulsky, *et al.*, "A model to compute phase diagrams in oxides with empirical or first-principles energy methods and application to the solubility limits in the CaO–MgO system," *J. Am. Ceram.*, 49, 2033, 1996.